Hyperoxia impairs induced pluripotent stem cell-derived endothelial cells and drives an atherosclerosis-like transcriptional phenotype

Sean M. Carr, PhD,[a,b] Katherine Owsiany, MD, PhD,[a,b] Ottis Scrivner, PhD,[a,b] Dylan McLaughlin, MD,[a,b] Hanjoong Jo, PhD,[a,c] Luke P. Brewster,[a,b,c] *and* Katherine E. Hekman, MD, PhD,[a,b] *Atlanta and Decatur, GA*

ABSTRACT

Background: Induced pluripotent stem cells (iPSCs) directed to endothelial identity (iPSC-ECs) are emerging as a potent tool for regenerative medicine in vascular disease. However, iPSC-ECs lose expression of key identity markers under standard in vitro conditions, limiting their clinical applications.

Methods: To model physiological in vivo conditions, we examined the bioenergetics, presence of key cell markers, and proliferative and angiogenic capacity in iPSC-ECs at late and early passage under hyperoxic (21%) and physiological (4%) oxygen concentrations.

Results: Physoxia resulted in relative preservation of mitochondrial bioenergetic activity, as well as CD144 expression in late passage iPSC-ECs, but not proliferative capacity or tube formation. Single cell RNA sequencing (scRNA-seq) revealed that late passage hyperoxic iPSC-ECs develop an endothelial-to-mesenchymal phenotype. Comparing scRNA-seq data from iPSC-ECs and from atherosclerotic ECs revealed overlap of their transcriptional phenotypes.

Conclusions: Taken together, our studies demonstrate that physiological 4% oxygen culture conditions were sufficient to improve mitochondrial function in high passage cells, but alone was insufficient to preserve angiogenic capacity. Furthermore, late passage cells under typical conditions take on an endothelial-to-mesenchymal phenotype with similarities to ECs found in atherosclerosis. (JVS—Vascular Science 2024;5:100193.)

Keywords: Induced pluripotent stem cells; Regenerative medicine; Peripheral arterial disease; Endothelial cells; Hypoxia; Physoxia; Atherosclerosis

Patient-specific endothelial cells and vascular tissue derived from induced pluripotent stem cells (iPSC-ECs) are of major interest in the field of regenerative medicine and represent a promising treatment for severe peripheral arterial disease (PAD). However, cellular senescence in culture is a major limitation, because iPSC-ECs lose their characteristic markers and exhibit decreased proliferation after an average of 2 weeks.[1] During development and in the stem cell niche, differentiating endothelial cells experience a relatively hypoxic environment of 5% to 10% oxygen (termed physoxia), compared with the 20% atmospheric oxygen environment in most cell culture incubators. Multiple studies have shown that physoxia is critical for EC development in vivo and during EC differentiation from iPSCs in vitro.[2,3] However, the role of oxygen concentration after the differentiation period to maintain iPSC-EC identity remains unexplored.

In our previous work, we showed that iPSC differentiating to EC underwent mitophagy, a specialized subset of autophagy that governs mitochondrial breakdown and recycling within the cell.[4] We also showed that stimulating autophagy through the use of adenosine monophosphate kinase activator RG2 improved proliferative capacity of iPSC-ECs. Moreover, the proliferative capacity of embryonic stem cells correlates with reduced mitochondrial oxygen consumption, whereas differentiation is associated with an increase in reactive oxygen species and autophagy as a quality control mechanism.[5] However, the link between mitochondrial bioenergetic changes that may drive iPSC-EC identity and function remain inconclusive. In addition, iPSC-ECs are known to have significant heterogeneity,[6] but these populations have never been explored after multiple passages or compared with ECs found in relevant human disease states including atherosclerosis.

In this study, we hypothesize that growing iPSC-EC in 4% oxygen would improve the retention of endothelial cell identity. To test this hypothesis, we performed assays testing marker retention, senescence, and angiogenesis of iPSC-ECs grown in 4% versus 20% oxygen and early versus late passage. Our results show that culturing iPSC-EC to late passage in physoxia preserves bioenergetic capacity, but that these cells were not superior in proliferation or angiogenic capacity by sprouting assays compared with hyperoxic cells. By single cell transcriptomics, hyperoxic iPSC-ECs express a transcriptional program consistent with endothelial-to-mesenchymal

From the Department of Surgery, Emory University School of Medicine, Atlanta[a]; the Atlanta VA Healthcare System, Surgical and Research Services, Decatur[b]; and the Wallace H Coulter Department of Biomedical Engineering, Georgia Institute of Technology and Emory University, Atlanta.[c]

SC and KO contributed equally to this article and share co-first authorship.

Correspondence: Hekman Katherine E., MD, PhD, 1365 Clifton Rd NE Building A, Atlanta Georgia 30322 (e-mail: kowsian@emory.edu).

The editors and reviewers of this article have no relevant financial relationships to disclose per the Journal policy that requires reviewers to decline review of any manuscript for which they may have a conflict of interest.

2666-3503

https://doi.org/10.1016/j.jvssci.2024.100193

(EndMT) and bear resemblance to atherosclerotic ECs from in vivo disease models.

METHODS

Cell culture. iPSC lines ACS1028 and Y6 were obtained, cultured, and differentiated to ECs as described previously.[4,7] Early passage cells were defined as the first and second passage after CD144 bead purification, and late cells were defined as 2 weeks beyond the early stage. Hyperoxic cells were grown in a standard tissue culture incubator with 21% O_2. Physiological oxygen samples were maintained in 4% O_2 in a hypoxia chamber (Stem Cell Technologies, Vancouver, Canada; #27310). iPSC-ECs were treated with 1 μM of UK5099 (SigmaPZ0160; Sigma-Aldrich, St. Louis, MO) or vehicle control for 24 hours.

Mitochondrial bioenergetics. The Mito Stress Test Kit (Agilent Technologies, Santa Clara, CA; 103010-100) and Glycolysis Stress Test Kit (Agilent 103020-100) were performed on a Seahorse Analyzer. Mitochondrial stress test base media was 1 mmol/L pyruvate, 2 mmol/L glutamine, and 10 mmol/L glucose. Mitochondrial stress test assay was 1.5 μmol/L oligo then 1μmol/L FCCP then 0.5 μmol/L Rot/AA. Glycolysis stress test base media was 2 mmol/L glutamine. Runs were performed as 3 minutes mix and 3 minutes wait. Glycolysis stress test assay was 10 mmol/L glucose then 1 μmol/L oligo then 50 mmol/L 2 dg. Both assays were run for 3 minutes each for mix, wait, and read. Data were normalized to the total protein content determined by a bicinchoninic acid assay.

Single cell RNA sequencing data analysis. Gene-barcode matrices were analyzed in R using Seurat v4.3.0. Cells were filtered for 1000 to 9000 reads per UMI, ≤10% mitochondrial gene content. Clusters were calculated with 30 PCs at a resolution on 0.5. iPSC data and atherosclerotic data were filtered for gene and mitochondrial content as described and normalized before being combined using integrated multimodal analysis. The SingleR package v2.0.0 was also used to explore unsupervised annotation of clusters. Data from murine atherosclerotic plaque lineage traced for CDH5 was obtained from Alencar et al.[8] at GSM4555602. and from Zhao et al.[9] at GSE169332. Data from human atherosclerotic plaque was obtained at GSE155512. Raw data from Y6 cells is available at GSE63090 and code are available upon request.

Data analysis and statistics. There were three biological replicates for each group in each experiment, unless otherwise specified. For comparison of multiple groups, we performed one-way or two-way analysis of variance followed by the Tukey method of multiple pairwise comparisons. A P value of $<.05$ was considered significant.

RESULTS

ECs in vivo experience roughly 5% oxygen tension, yet are routinely cultured under standard 21% oxygen conditions. Given the relationship between mitochondrial accumulation and decreased iPSC-EC function, we sought to investigate whether the standard 21% O_2 culture condition was affecting mitochondrial function through presumed oxidative stress.

We performed Seahorse assays on our Y6 iPSC-ECs grown under conditions of physoxia (4%) or hyperoxia (21%) (experimental design in Supplementary Fig 1, online only). At early passage numbers, no difference was observed between groups in maximal response to mitochondrial or glycolytic stress test (Fig 1, *A*, *B*). Because ECs and particularly angiogenic tip cells favor glycolysis, we empirically titrated and treated cells with a mitochondrial pyruvate transporter inhibitor, UK5099, to block mitochondrial respiration and theoretically shunt energy production toward glycolysis. Cells treated with UK5099 showed a decrease in mitochondrial respiration, consistent with previous data, but overall did not demonstrate a significant impact on glycolytic function (Fig 1, *A*, *B*).[10] In late passage ECs, cells grown at a physiological oxygen concentration had preserved bioenergetics throughout the mitochondrial stress test, which was lost when continuously cultured with UK5099 (Fig 1, *C*). Cells cultured in physoxia also had elevateds maximal rates of glycolysis, which surprisingly was again lost when continuously cultured in the presence of UK5099 (Fig 1, *D*). These findings were replicated in an independent cell line, ACS1028-derived iPSC-EC (Supplementary Fig 2, online only). These data support the conclusion that cellular metabolic capacity for both respiration and glycolysis is profoundly enhanced by physiological conditions, especially after multiple passages.

Because physiological oxygen levels during differentiation have been shown to enhance EC identity in iPSC-derived cells, we examined the effect of continuous culture under physoxia (4%) and hyperoxia (21%) on the retention of markers of EC identity. Immunofluorescence microscopy showed that early passage cells grown in physoxia or hyperoxia expressed CD144 (Fig 2, *A*, *B*). In contrast, after culture for 2 weeks in hyperoxia or physoxia, we found that CD144 and CD31 were preferentially retained on cells cultured in 4% O_2 with or without UK5099 treatment (Fig 2, *C-E*). Cells grown in physoxia retained 70% of CD31 and 60% of CD144, compared with only 45% and 38% retention of CD31 and CD144 in hyperoxia grown cells, respectively. These data support the conclusion that physiological oxygen levels allow late passage iPSC-ECs to retain their characteristic markers.

Next, we investigated the effect of physoxia on survival, senescence, and EC function. As expected, high passage cells showed greater senescence quantified by ß-galactosidase assay (27% high passage vs 16.5% low passage) (Fig 3, *A*); this was not significantly affected by oxygen concentration, consistent with previous observations.[4] Physoxia did not preserve proliferative capacity

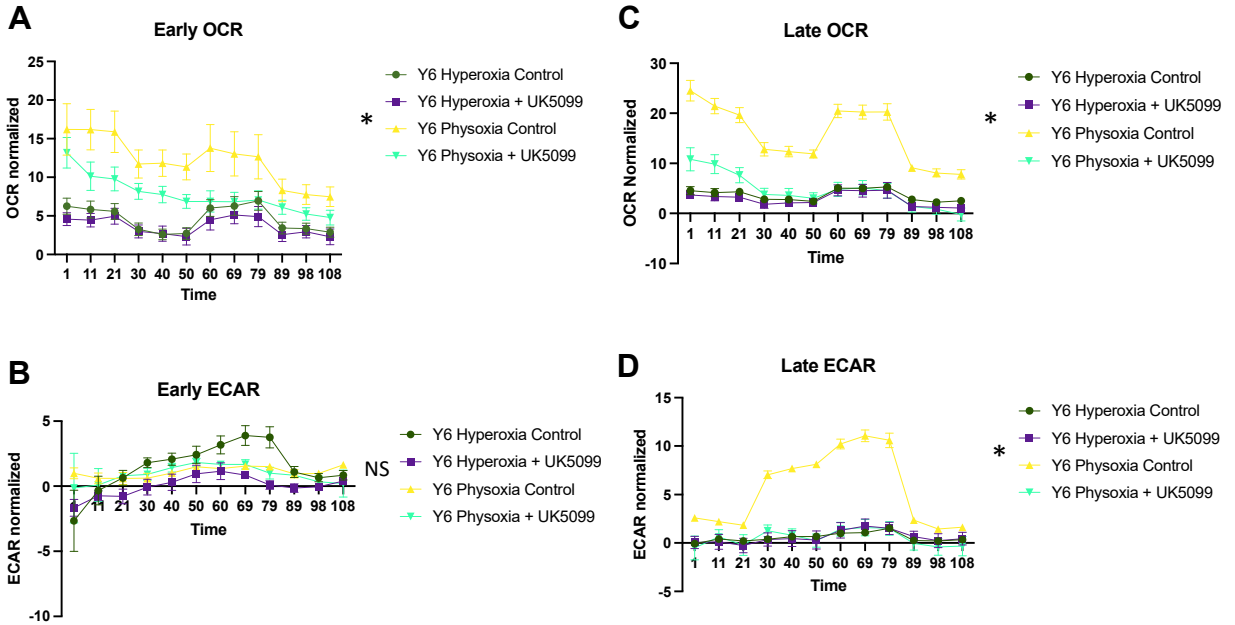

Fig 1. Physiological oxygen (physoxia) enhances mitochondrial respiration and glycolysis in late passage induced pluripotent stem cells directed to endothelial identity (iPSC-ECs). Y6 iPSC-derived endothelial cells on passage 3 (early) or 8 (late) were subjected to a Seahorse metabolic analysis with mitochondrial stress test (MST) or glycolysis stress test (*GST*). **(A)** MST for cells grown under physoxia (4% oxygen) or hyperoxia (21% oxygen), with or without addition of pyruvate transport inhibitor UK5099. **(B)** Glycolytic stress test curve for the samples in **(A)**. **(C)** MST for late passage cells grown under physoxia or hyperoxia, with or without UK5099 treatment. **(D)** GST curve for cells in **(C)**. *$P < .05$ by two-way analysis of variance testing with correction for multiple comparisons. Error bars in all frames show standard error of three technical replicates. The graph images are one of two independently conducted experiments. *ECAR*, extracellular acidification rate; *OCR*, oxygen consumption rate.

compared with hyperoxia in higher passage cells (Fig 3, *B*). To examine how function is affected by physoxia, we examined nitric oxide synthase (NOS) activity and angiogenic capacity by an in vitro sprouting assay. Total NOS activity was higher in hyperoxic conditions (Fig 3, *C*). However phosphorylated endothelial NOS was higher in physoxia, implying that hyperoxic cells had higher inducible NOS contributing to the total NOS production, which is a known marker of cellular stress[11] (Fig 3, *D, F*). The addition of UK5099 also did not have an effect on senescence, proliferation or NOS activity. Finally, late passage cells showed higher endothelial tube formation compared with early passage cells, with significant increases in junction formation (an average of 106 junctions in late control vs 25 in early control) (Fig 3, *E, G*), suggesting that early passage cells possess immature EC functions. Somewhat surprisingly, culture at physoxia did not improve these measures when compared with hyperoxia (106 junctions in late hyperoxia vs 71 junctions in late physoxia). Taken together, these data show that, although physoxia had a favorable effect on mitochondrial bioenergetics and on endothelial marker retention in late passage cells, proliferation and angiogenic function were not enhanced.

To better understand the heterogeneity in our population of late passage iPSC-ECs, we performed single cell RNA sequencing (scRNA-seq) of high passage cells cultured under 21% oxygen conditions. Surprisingly, despite selecting for CD144 (aka *CDH5*)-positive cells by magnetic bead sorting after differentiation, a substantial proportion of cells lacked expression of this marker after 2 weeks in culture (Supplementary Fig 3, online only) and many cells expressed a gene signature with multiple collagens (*Col1a1*, *Col1a2*, *Col6a1*, and *Col6a2*) and mesenchymal markers (*Pdgfrb*, *Fbn1*, *Tgfbr1*, and *Vegfa)* reminiscent of studies involving *CDH5*-lineage traced ECs in murine atherosclerosis.[8] To critically assess the overlap between iPSC-ECs and atherosclerotic ECs, scRNA-seq data from *CDH5*^{hi} Y6 iPSC-ECs and lineage-traced atherosclerotic ECs were clustered together using integrated multimodal analysis in Seurat (Fig 4, *A*). This approach yielded 8 clusters with top genes shown in Fig 4, *B*. All clusters had strong expression of *CDH5* and *PECAM1*, confirming they were canonical ECs (Fig 4, *D*). The atherosclerosis-derived cells were predominantly found in cluster 3, but also contributed to cluster 1 and cluster 4, with 57% of cells ultimately overlapping with iPSC-ECs (Fig 4, *B, C*). Atherosclerosis-derived cells expressed multiple markers found in iPSC-ECs, including conventional markers like *Cdh5*, *Pecam1*, and *EphB4*, as well as *CD34* and colony forming markers *Mcam* and *Eng* (Fig 4, *E, F*). Strong overlap was also seen in clusters

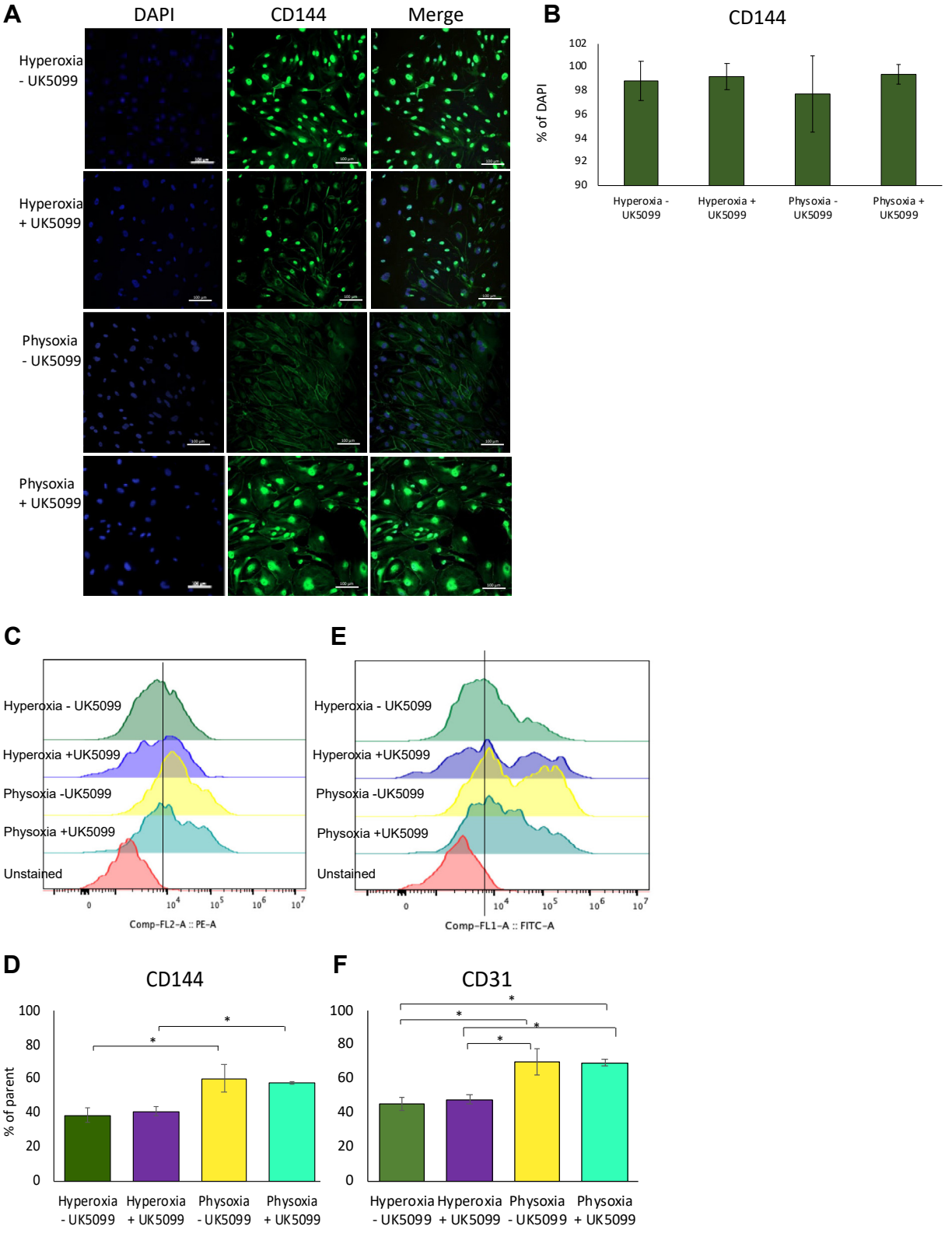

Fig 2. Induced pluripotent stem cells directed to endothelial identity (iPSC-ECs)grown at physoxia show enhanced endothelial marker retention in late passages. **(A)** Early passage iPSC-ECs grown under hyperoxia or physoxia with and without addition of UK5099 were immunostained for CD144 and DAPI and imaged with confocal microscopy. Representative images from each group are shown along with all channels alone or merged. Original magnification 20× with scale bars showing 100 μm. DAPI is blue, CD144 is green. **(B)** Quantification of $CD144^+$ cells/$DAPI^+$ cells from two independent replicates. **(C)** Late passage Y6 iPSC-EC grown under physoxia or hyperoxia with or without addition of UK5099 were fixed, immunostained for CD31 and

1 and 3, which were defined by markers of EndMT, including *Vcam1*, *Acta2*, *Vim*, and *Tgfb1*, as well as *Col4a*.

We also examined the broader population of late passage iPSC-ECs, beyond the *CDH5*^{hi} subpopulation (Supplementary Fig 3, online only). Unsupervised annotation of the clusters with SingleR included labels such as tissue stem cells, smooth muscle cells, or mesenchymal stem cells, although cells classified as ECs contributed to all populations (Supplementary Fig 3, *B* and *C*, online only). Notably, there were no cells classified as fibroblasts in our data. Co-clustering the broader iPSC-EC population with the Alencar et al.[8] lineage-traced murine atherosclerotic EC data corroborated the trend of overlap between late passage iPSC-ECs and atherosclerotic ECs (Supplementary Fig 3, *D-F*, online only). To further validate these findings, we compared our total late passage iPSC-EC population to a distinct dataset derived from CD31^{+} purified ECs isolated from murine atherosclerotic plaque published by Zhao et al.[9] and found similar results (Supplementary Fig 4, online only). Finally, we compared our iPSC-EC scRNA-seq data to a published dataset of human carotid artery plaque from Pan et al,[12] which demonstrated significant overlap in clusters 1 through 4, with shared expression of multiple markers of EndMT as well as CD34 (Supplementary Fig 5, online only). Overall, 80% of cells were in clusters shared between iPSC-EC and plaque EC, and 48% of cells were in clusters with >5% overlap.

We also chose three EndMT markers from our scRNA-seq data (COL1A1, COL4A1, and vimentin) for validation with Western blotting (Fig 4, *G*) and comparison with our iPSC-EC cultured under hypoxia vs physoxia for 2 weeks. Results show a consistent downtrend in all three markers, supporting the hypothesis that the EndMT phenotype observe in the late hyperoxic samples is decreased under physoxic conditions.

Taken together, these data support the hypothesis that there is similarity between a subset of long-term culture aged iPSC-ECs and ECs found in atherosclerosis, including a population undergoing an EndMT transition.

DISCUSSION

In our study we observed that (1) iPSC-ECs aged through multiple passage lose not only their characteristic markers, but also lose bioenergetic function which was improved by culture in physoxia (4%), although this did not correlate with enhanced function relative to hyperoxia; and (2) aged iPSC-EC transcriptomic profiling resembles murine atherosclerotic lineage-traced ECs and human atherosclerotic ECs. As key regulators of angiogenesis, ECs are exquisitely sensitive to oxygen concentration; however, most tissue culture incubators are maintained at 21% oxygen, consistent with the atmosphere, but not the oxygen concentration experienced by ECs in the body. Values of oxygenation in interstitial tissue vary, gradually decreasing from the lungs to distal organs, ranging from 11% to 1%.[13] Healthy muscle tissue has approximately 3.4% oxygen at rest, whereas patients with PAD have reduced hemoglobin saturation of oxygen with exercise.[13,14] Further, oxygen concentration in stem cell niches is 2% to 9% with sharp local gradients, and oxygen concentration has been shown to be crucial to stem cell proliferation, metabolism, and cell signaling.[15,16] Thus, culture at physiological oxygen levels is not only of value in promoting cellular proliferation, metabolism, and marker expression in our study, but also has relevance in the human disease cycle of normoxia, ischemia, and reoxygenation.

We previously showed that 1.5% oxygen prevents accumulation of mitochondria in iPSC-ECs and transiently stimulates proliferation; however, over time these cells still demonstrated senescence and loss of proliferation.[4] Here, we show that physoxia restores bioenergetic function, consistent with previous observations that it improves abnormal accumulation of mitochondria. However, physiological oxygen concentrations did not prevent senescence, restore proliferative capacity or improve angiogenic sprouting in late passage cells. Although initially surprising, the results of our scRNA-seq transcriptomic profiling shed some light on the subject. Our iPSC-ECs under standard conditions express markers of EndMT. Although essential for the growth of heart valves and vascular structures during development, the process in adults is largely associated with a dysfunctional response to disease processes, and increasing amounts of EndMT correlate with clinical disease severity.[17] EndMT shares many regulators and pathways with angiogenesis including transforming growth factor β, vascular endothelial growth factor, and hypoxia-inducible factor 1-alpha, so much so that angiogenesis has been called a partial EndMT.[18] Seemingly enhanced angiogenic sprouting of iPSC-ECs under 21% oxygen conditions may reflect the similarities between angiogenic and EndMT process, whereas iPSC-ECs under physoxia are more akin to quiescent ECs. This is evident in our data, in which cluster 3, enriched for markers of EndMT,

underwent flow cytometry. A mixture of all cells unstained were used as a negative control. **(B)** Representative ridge plots showing physoxia grown samples retaining CD144. **(D)** Quantification of CD144-positive cells in experiment in **(C)**. **(E)** Cells from **(B)** were also stained with CD31 and assessed by flow cytometry. Ridge plot showing expression of CD31, which was retained in late passage cells grown under physoxia. **(F)** Quantification of CD31-positive cells from experiment in **(E)**. Error bars show ± SE among three technical replicates. *$P < .05$ with Student's *t* test.

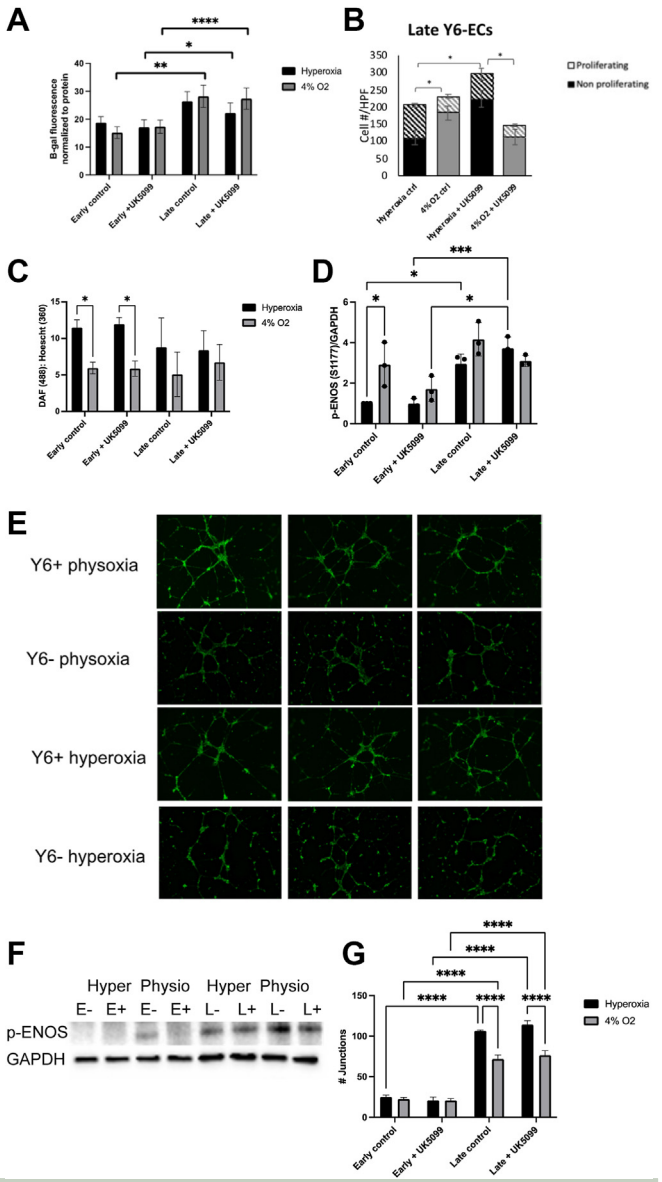

Fig 3. Induced pluripotent stem cells directed to endothelial identity (iPSC-ECs) sub-culturing results in senescence and functional loss not ameliorated by physoxia. **(A)** iPSC-ECs grown to early or late passage under hyperoxia or physoxia was treated (+) with UK5099 or untreated (−) and subjected to beta-galactosidase assay to assess cell senescence. Late passage cells showed greater senescence in both physoxia and hyperoxia groups. Graph shows beta galactosidase normalized to total protein per well. **(B)** Cells from experiment in **(A)** were also treated with fluorescent EdU to assess proliferation. Graph shows the number of cells proliferating and not proliferating in each group **(C)**. Cells from the experiment in **(A)** were tested for total nitric oxide synthase (NOS) activation, quantified as DAF normalized to Hoechst staining. **(D)** Cell lysates from the experiment in **(C)** were probed with specific antibody to phosphorylated endothelial NOS and quantified by Western blotting. **(D)** Cell lysates from the experiment in (**C**) were probed with specific antibody to phosphorylated eNOS and quantified by Western blotting. **(E)** Cells from experiment in **(A)** were exposed to Matrigel matrix for 16 hours and analyzed for endothelial tube formation. Representative images from each condition imaged with fluorescence microscopy are shown. Lens: 20x; zoom: ×1. **(F)** Representative images from Western blot quantified in **(D)**. **(G)** Experiment in **(E)** was quantified for the number of junctions between tube structures in ImageJ. Error bars show ± SE in three independent experiments. $^{*}P < .05$; $^{**}P < .01$; $^{***}P < .005$; $^{****}P < .001$.

is also defined by collagen 4a, which is associated with angiogenesis.[19]

Although most of our assays model the regenerative capacity of ECs in the microvascular setting, we sought to understand how our populations modeled the state of macrovascular disease by comparing our populations to published datasets of scRNA-seq of atherosclerotic plaque in animal models. Several populations of iPSC-ECs have been previously described, including early (*CD34 Klf2 Ecscr* positive), late (*Cdh5*, *Erg*, *Flt1*, and *KDR* positive), and activated (*Esm1*) populations.[6] These populations were present in our data, but our analysis extended further to show that some iPSC-EC take on a phenotype similar to cells found in atherosclerosis, with most overlap found in a population defined by mesenchymal markers. Several scRNA-seq studies in the setting of atherosclerosis provide evidence of this transcriptional program, consisting of collagens, fibronectin, and transforming growth factor β expression.[8,9,20] ECs are known to undergo an EndMT transition in atherosclerosis, as well as participate in neoangiogenesis within atherosclerotic lesions; however, these transitions are largely considered maladaptive. Our studies show overlap between an EndMT transition in aged cells and the transcriptional profile of ECs in atherosclerosis. These results support the relevance of our model to the atherosclerotic component of PAD, but also highlight a potential pitfall to using aged iPSC-ECs as a treatment, because they are subject to the same maladaptive responses. Future studies would be needed to investigate the potential benefit of physoxia and additional optimized culture conditions on the transcriptomic profile of iPSC-ECs.

CONCLUSIONS

In our studies, we explored the bioenergetic function, cellular identity, and function of iPSC-ECs aged through high passage and under physiological oxygen conditions. Physoxia was sufficient to improve mitochondrial function in high passage cells and helped cells maintain CD144 marker expression. However, cells grown in hyperoxia still displayed a higher degree of proliferation and angiogenic capacity. This finding is in part explained by our finding that some aged cells under typical conditions take on an EndMT phenotype with similarities to ECs found in the diseased state of atherosclerosis.

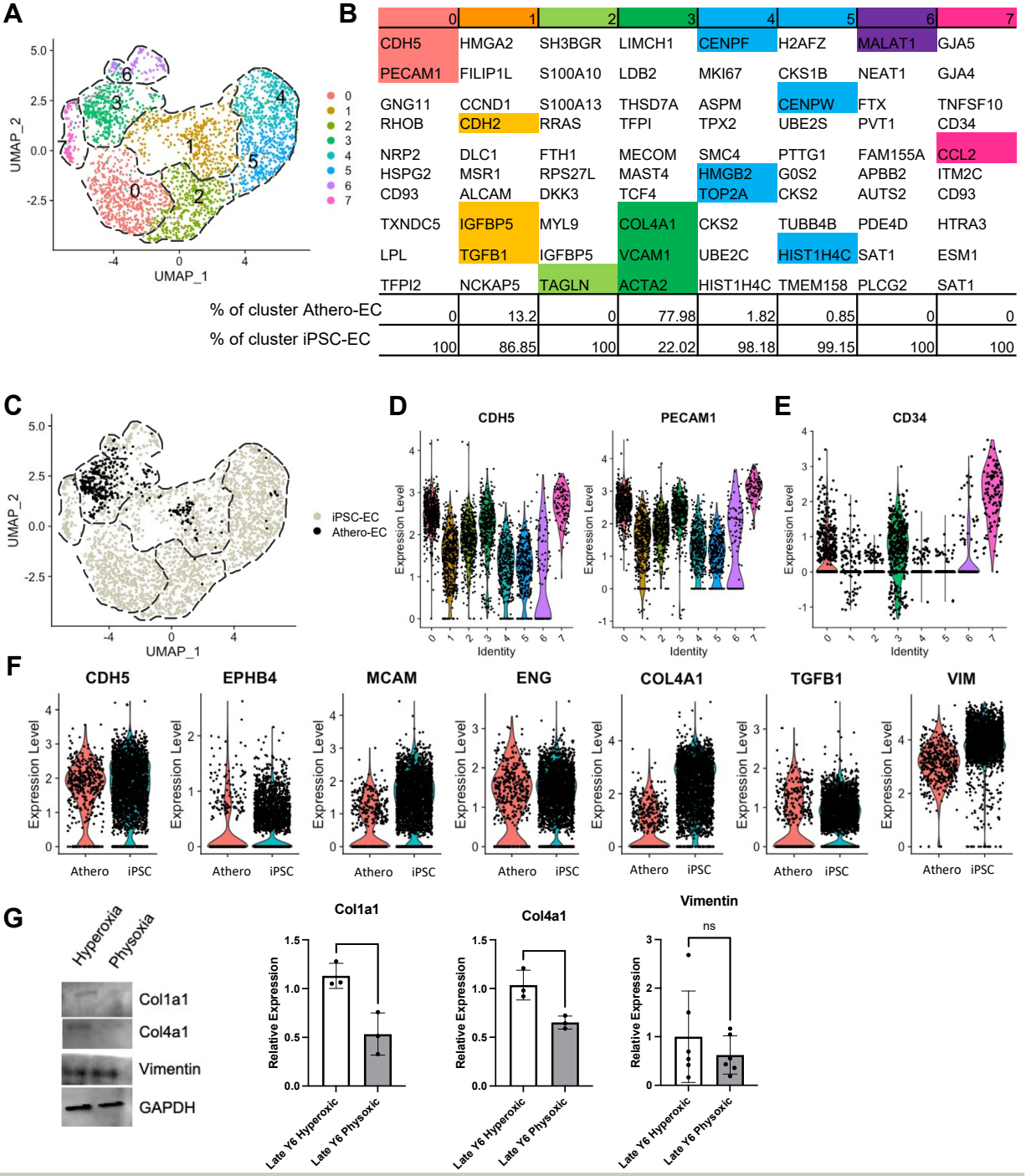

	0	1	2	3	4	5	6	7
	CDH5	HMGA2	SH3BGR	LIMCH1	CENPF	H2AFZ	MALAT1	GJA5
	PECAM1	FILIP1L	S100A10	LDB2	MKI67	CKS1B	NEAT1	GJA4
	GNG11	CCND1	S100A13	THSD7A	ASPM	CENPW	FTX	TNFSF10
	RHOB	CDH2	RRAS	TFPI	TPX2	UBE2S	PVT1	CD34
	NRP2	DLC1	FTH1	MECOM	SMC4	PTTG1	FAM155A	CCL2
	HSPG2	MSR1	RPS27L	MAST4	HMGB2	G0S2	APBB2	ITM2C
	CD93	ALCAM	DKK3	TCF4	TOP2A	CKS2	AUTS2	CD93
	TXNDC5	IGFBP5	MYL9	COL4A1	CKS2	TUBB4B	PDE4D	HTRA3
	LPL	TGFB1	IGFBP5	VCAM1	UBE2C	HIST1H4C	SAT1	ESM1
	TFPI2	NCKAP5	TAGLN	ACTA2	HIST1H4C	TMEM158	PLCG2	SAT1
% of cluster Athero-EC	0	13.2	0	77.98	1.82	0.85	0	0
% of cluster iPSC-EC	100	86.85	100	22.02	98.18	99.15	100	100

Fig 4. CDH5^{hi} late passage induced pluripotent stem cells directed to endothelial identity (iPSC-ECs) bear similarity to atherosclerotic ECs. **(A)** CDH5-expressing populations from our late Y6 iPSC-derived EC scRNA-seq dataset were isolated and clustered with previously published, lineage-traced atherosclerotic murine ECs using integrated multimodal analysis in Seurat. Resulting UMAP shown in **(A)**. **(B)** Top 10 marker genes for each cluster in **(A)**. **(C)** UMAP plot showing overlap between atherosclerotic ECs (black) and CDH5^{hi} iPSC-ECs (gray) **(D)**. Violin plots showing expression of CDH5 and PECAM1 across the dataset **(E)**. Violin plot of CD34, with clusters 3 and 7 showing high expression. **(F)** Expression of EC stem markers and EndMT markers were compared between atherosclerotic cells and Y6 iPSC-ECs, showing comparable expression in both datasets. **(G)** Whole cell lysates from early and late iPSC-ECs cultured under hyperoxia or physoxia were probed for protein expression of Col1a1, Col4a1, and vimentin by Western blotting. Representative blots are followed by plots of quantified expression in each condition normalized to GAPDH. Each experiment consisted of three biological and three technical replicates.

FUNDING

This work was funded by the Atlanta VA Healthcare System Career Development Award (K.E.H.), the American College of Surgeons Faculty Research Fellowship (K.E.H.), the Doris Duke Foundation Program for Retaining, Supporting and Elevating Early-career Researchers at Emory UL1-TR002378 (K.E.H.), the Vascular and Endovascular Surgical Society Early Career Investigator Award (K.E.H.), the Department of Veterans Affairs Small Projects in Rehabilitation RR&D I21 RX004399 (K.E.H. and S.M.C.), NHLBI RO1 HL143348 (L.B.), Veteran Affairs BLR&D IO1BX004707 (L.B.), and Vascular Fellowship from Joseph Maxwell Cleland Atlanta VA Medical Center (K.O., and D.M.). Research reported in this publication was supported by the Emory Integrated Genomics Core Shared Resource of Winship Cancer Institute of Emory University and NIH/NCI award P30CA138292. The content is solely under the responsibility of the authors and does not represent the official views of the National Institutes of Health.

DISCLOSURES

None.

REFERENCES

1. Li Z, Hu S, Ghosh Z, Han Z, Wu JC. Functional characterization and expression profiling of human induced pluripotent stem cell- and embryonic stem cell-derived endothelial cells. *Stem Cells Dev*. 2011;20:1701–1710.
2. Podkalicka P, StÎ Epniewski J, Mucha O, Kachamakova-Trojanowska N, Dulak J, Łoboda A. Hypoxia as a driving force of pluripotent stem cell reprogramming and differentiation to endothelial cells. *Biomolecules*. 2020;10:1614.
3. Kusuma S, Peijnenburg E, Patel P, Gerecht S. Low oxygen tension enhances endothelial fate of human pluripotent stem cells. *Arterioscler Thromb Vasc Biol*. 2014;34:913–920.
4. Hekman KE, Koss KM, Ivancic DZ, He C, Wertheim JA. Autophagy enhances longevity of induced pluripotent stem cell-derived endothelium via mTOR-independent ULK1 kinase. *Stem Cells Transl Med*. 2022;11:1151.
5. Guan J-L, Simon AK, Prescott M, et al. Autophagy in stem cells. *Autophagy*. 2013;9:830–849.
6. Paik DT, Tian L, Lee J, et al. Large-scale single-cell RNA-seq reveals molecular signatures of heterogeneous populations of human induced pluripotent stem cell-derived endothelial cells. *Circ Res*. 2018;123:443–450.
7. Patsch C, Challet-Meylan L, Thoma EC, et al. Generation of vascular endothelial and smooth muscle cells from human pluripotent stem cells. *Nat Cell Biol*. 2015;17:994–1003.
8. Alencar GF, Owsiany KM, Karnewar S, et al. Stem cell pluripotency genes Klf4 and Oct4 regulate complex SMC phenotypic changes critical in late-stage atherosclerotic lesion pathogenesis. *Circulation*. 2020;142:2045–2059.
9. Zhao G, Lu H, Liu Y, et al. Single-cell transcriptomics reveals endothelial plasticity during diabetic atherogenesis. *Front Cell Dev Biol*. 2021;9:689469.
10. Zhong Y, Li X, Yu D, et al. Application of mitochondrial pyruvate carrier blocker UK5099 creates metabolic reprogram and greater stem-like properties in LnCap prostate cancer cells in vitro. *Oncotarget*. 2015;6:37758–37769.
11. Cinelli MA, Do HT, Miley GP, Silverman RB. Inducible nitric oxide synthase: regulation, structure, and inhibition. *Med Res Rev*. 2020;40:158.
12. Pan H, Xue C, Auerbach BJ, et al. Single-cell genomics reveals a novel cell state during smooth muscle cell phenotypic switching and potential therapeutic targets for atherosclerosis in mouse and human. *Circulation*. 2020;142:2060–2075.
13. Carreau A, Hafny-Rahbi B El, Matejuk A, Grillon C, Kieda C. Why is the partial oxygen pressure of human tissues a crucial parameter? Small molecules and hypoxia. *J Cell Mol Med*. 2011;15:1239.
14. Comerota AJ, Throm RC, Kelly P, Jaff M, York N. Tissue (muscle) oxygen saturation (StO2): a new measure of symptomatic lower-extremity arterial disease. *J Vasc Surg*. 2003;38:724–729.
15. Spencer JA, Ferraro F, Roussakis E, et al. Direct measurement of local oxygen concentration in the bone marrow of live animals. *Nature*. 2014;508:269–273.
16. Haque N, Rahman MT, Hayaty N, Alabsi A. Hypoxic culture conditions as a solution for mesenchymal stem cell based regenerative therapy. *Sci World J*. 2013;2013:632972.
17. Bischoff J. Endothelial to mesenchymal transition — purposeful versus maladaptive differentiation. *Circ Res*. 2019;124:1163.
18. Welch-Reardon K, Wu N, Hughes C. A role for partial endothelial-mesenchymal transitions in angiogenesis? *ATVB*. 2015;35:303–308.
19. Chen L, Bai J, Li Y. miR-29 mediates exercise-induced skeletal muscle angiogenesis by targeting VEGFA, COL4A1 and COL4A2 via the PI3K/Akt signaling pathway. *Mol Med Rep*. 2020;22:661–670.
20. Cheng CK, Lin X, Pu Y, et al. SOX4 is a novel phenotypic regulator of endothelial cells in atherosclerosis revealed by single-cell analysis. *J Adv Res*. 2023;43:187.
21. Arnaoutova I, Kleinman HK. In vitro angiogenesis: endothelial cell tube formation on gelled basement membrane extract. *Nat Protoc*. 2010;5:628–635.

Submitted Oct 23, 2023; accepted Jan 22, 2024.

APPENDIX.

Supplemental Methods

Immunohistochemistry. Cells prepared as previously described and treated with primary (VE-cadherin/CD144 (Sigma-Aldrich V1514, 1:200) and secondary antibodies (Life Technologies, Carlsbad, CA, 1:300) Cells were imaged on a Nikon A1R upright fluorescence confocal microscope at an original magnification of 20x with 1× zoom.

Flow cytometry. For CD144 and CD31 (BD Biosciences, Franklin Lakes, NJ, 560410 and 560984, respectively), fixed cells were incubated with the conjugated primary antibody, 20 μL antibody for 1×10^6 cells in 100 μL of 1% bovine serum albumin/phosphate-buffered saline. Flow cytometry was performed on a Beckman Coulter (Brea, CA) Cytoflex cytometer and analyzed with FloJo v10.9.

β-Galactosidase assay. Fluorescence-based senescence β-galactosidase activity was performed with Cell Signaling Technology's (Danvers, MA) kit #23833 according to the manufacturer's instructions.

EdU proliferation. Proliferating cells were labeled with EdU using the Invitrogen (Carlsbad, CA) Click-iT microplate assay kit (Invitrogen C10214), without the use of the Amplex Ultra red step. Hoechst 33342 was added at 5 μg/mL (Invitrogen H1399), and labeled cells were imaged on a Keyence fluorescent plate imager BZ-X700. Images (original magnification ×4) were collected for each well of three biological replicates per condition. EdU-labeled and total nuclei were counted in Fiji.

Nitric oxide synthase production assay. Nitric oxide synthase activity was measured using the DAF-FM kit from Thermo Fisher Scientific (Waltham, MA; part number D23842) and read on a Syngene microplate reader in triplicate with an unlabeled control.

Tube formation assay. Endothelial tube formation assay was carried out as described in Arnaoutov and Kleinman.[21] Cells were examined 16 hours later and imaged on the Keyence fluorescent plate imager BZ-X700. Images were analyzed for tube length and branching with the AngioAnalyzer program in Fiji.

Western blotting. As previously described, Western blots were performed and probed with specific antibodies. Primary antibodies used as follows: GAPDH anti-rabbit polyclonal antibody (Millipore Sigma-Aldrich, G9545); anti-rabbit monoclonal p-ENOS S1177 (Cell Signaling Technology; 9570). Band intensities were measured and quantified by densitometry (GS-700 Imaging Densitometer; Bio-Rad, Hercules, CA). Quantification of Western blot was based on the ratio of the target protein to GAPDH.

Single cell RNA sequencing library preparation. Cells were digested to a single cell suspension, assessed for live cells >80%, and processed at the Emory Integrated Genomics Core using a 10× Genomics Chromium Controller device. The cDNA libraries were sequenced on Illumina NovaSeq 6000 to a depth of 15,000 UMI per cell. The Cell Ranger Single-Cell Software was used for demultiplexing, barcode processing, and alignment.

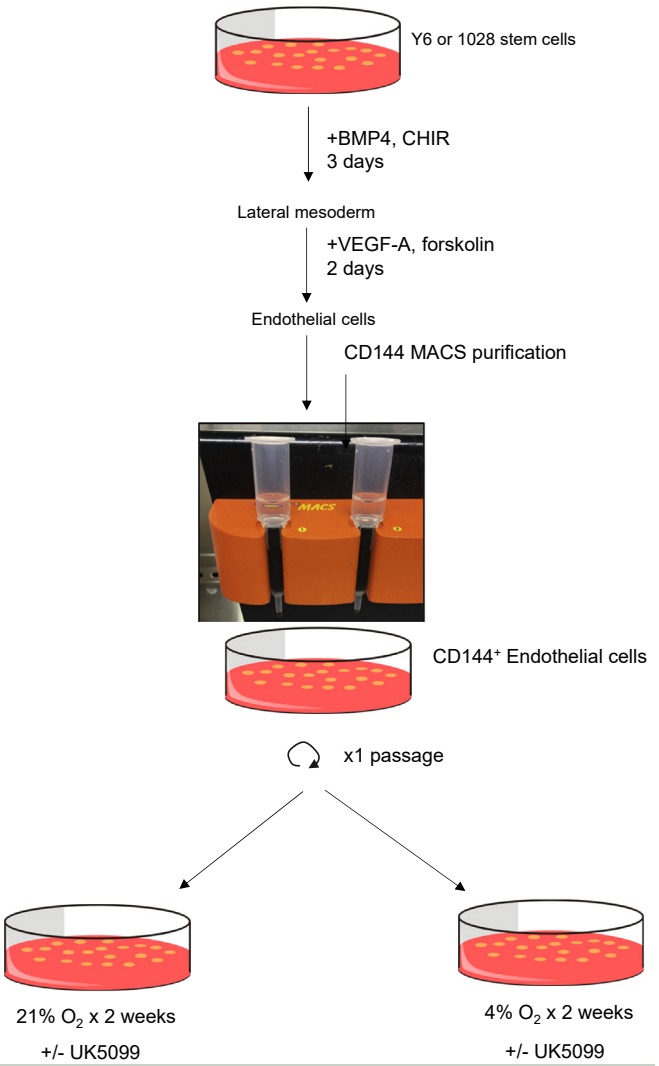

Supplementary Fig 1. Differentiation process and culture technique for induced pluripotent stem cells directed to endothelial identity (iPSC-ECs). Y6 or 1028 stem cell lines were differentiated to EC through a stepwise treatment with BMP4 and CHIR for 3 days followed by vascular endothelial growth factor A (*VEGF-A*) and forskolin supplementation for 2 days. $CD144^{+}$ cells were purified with magnetic beads and subcultured. After one passage, the cells were maintained in 4% oxygen (physoxia) or 21% oxygen (hyperoxia) for 2 weeks.

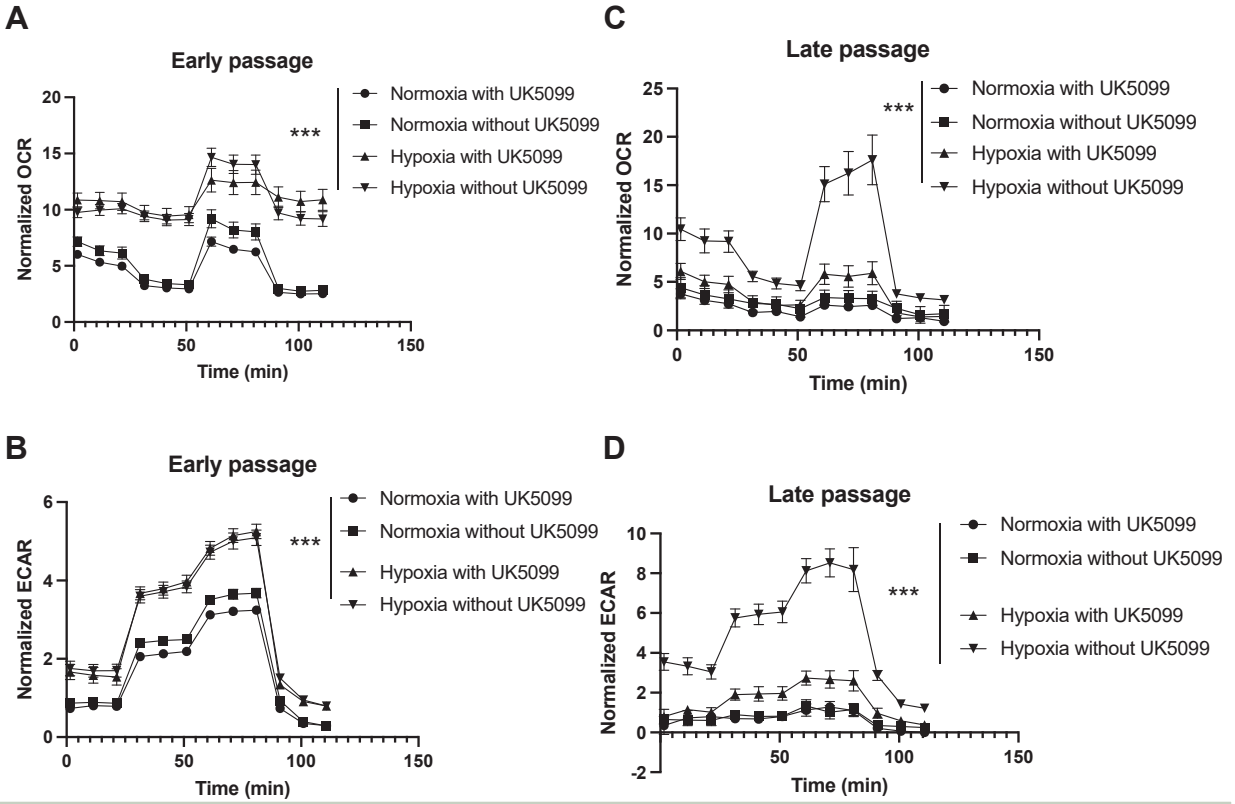

Supplementary Fig 2. Hypoxia preserves bioenergetic curves in late passage ACS1028-derived endothelial cells (ECs). **(A)** Mitochondrial stress (MST) curves for early passage ACS1028 cells. **(B)** Glycolysis stress test (GST) curves for late passage ACS1028-derived ECs. **(C)** MST curves for late passage ACS1028-derived ECs. **(D)** GST curves for ACS1028-derived ECs. Graph shows three independent replicate mean ± standard error. ***$P < .001$ by two-way analysis of variance with correction for multiple comparisons.

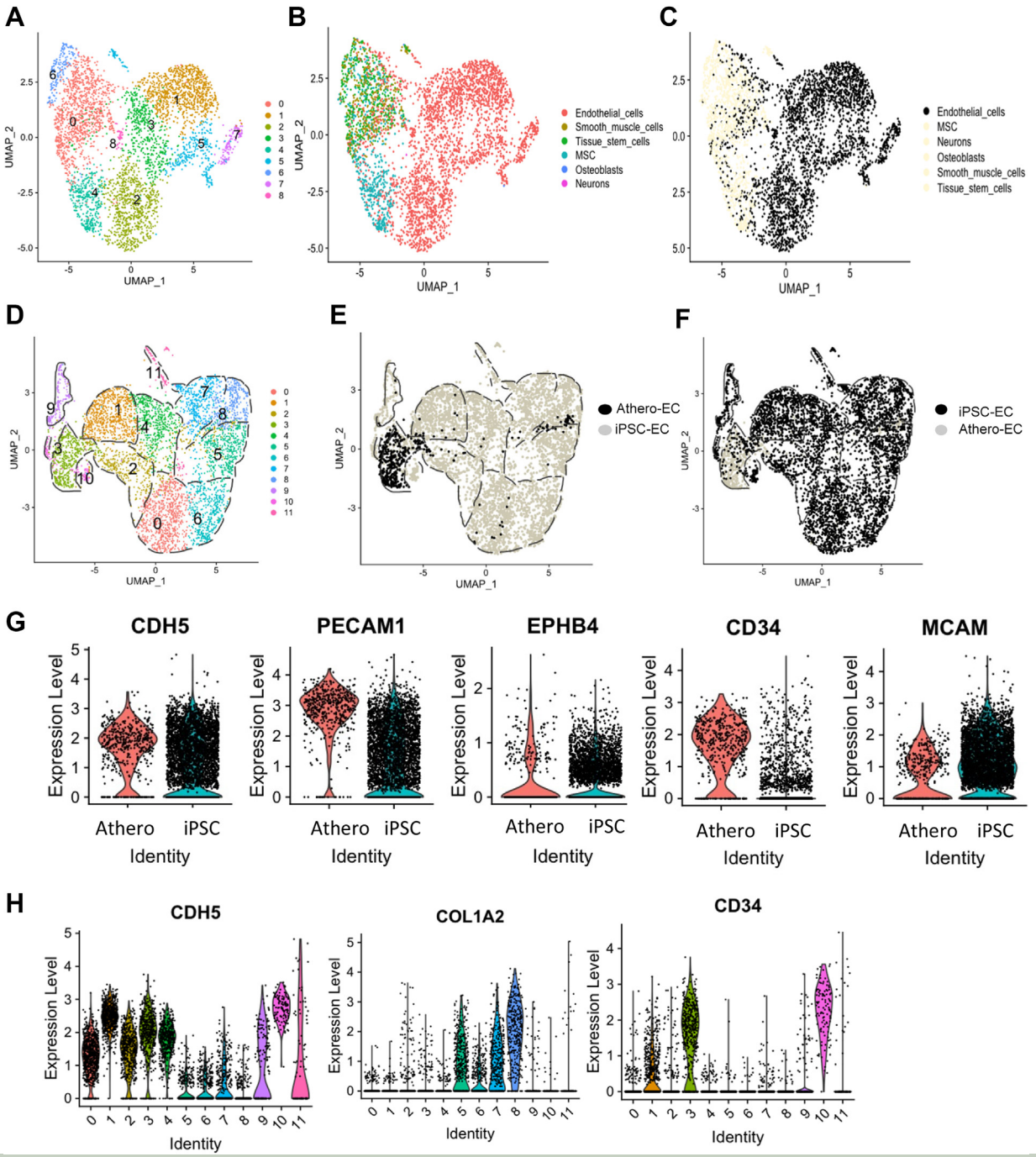

Supplementary Fig 3. Induced pluripotent stem cells directed to endothelial identity (*iPSC-ECs*) are similar to ECs derived from atherosclerotic plaque. **(A)** Late passage iPSC-ECs were sent for scRNA-seq. We analyzed 4116 cells after quality control. **(A)** UMAP of these cells with nine EC populations. **(B)** Late passage Y6 iPSC-ECs were annotated unsupervised with SingleR. **(C)** Plot from **(B)** with endothelial cells highlighted in black, showing unsupervised endothelial identity in all clusters. **(D)** The iPSC-EC dataset in **(A)** was combined with a dataset of lineage traced ECs from atherosclerotic plaques (extracted from Alencar et al 2020) using multimodal analysis to yield 11 total clusters. **(E)** Atherosclerotic ECs highlighted in black. **(F)** iPSC-EC highlighted in black. **(G)** Violin plots of select iPSC-EC genes also found in atherosclerotic samples. **(H)** Violin plots of genes defining clusters in **(A)**. CDH5 (clusters 0-2), CD34 (cluster 3), and Col1a2 (clusters 5-8).

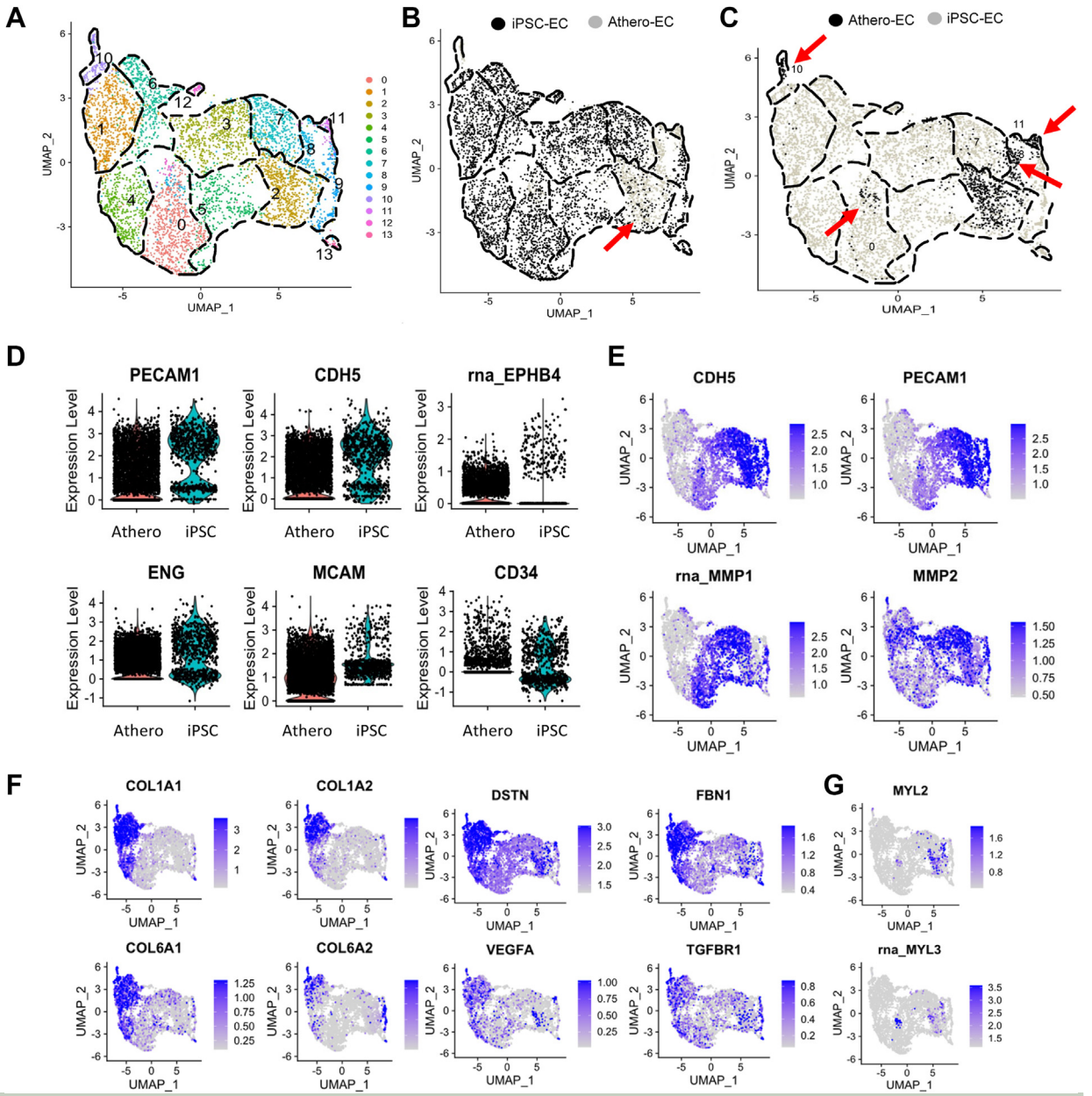

Supplementary Fig 4. Induced pluripotent stem cells directed to endothelial identity (*iPSC-ECs*) single cell RNA sequencing data were clustered with data from Western diet-fed diabetic mouse aorta and heart from Zhao et al. **(A)** Integrated UMAP clusters. **(B)** iPSC-EC highlighted, overlapping with atherosclerosis derived ECs in cluster 2. **(C)** Athero-derived ECs highlighted, with overlap in clusters 0, 8, 10, and 11. **(D)** Violin plots of EC marker genes expressed in both iPSC-EC and athero-EC datasets. **(E)** Feature plots of genes defining clusters 7-9 as activated endothelial cells. **(F)** Feature plots of collagens and EMT-related genes in clusters 1, 6, 10, and 11. **(G)** Feature plot of athero-EC cells from murine heart expressing Myl2 and Myl3.

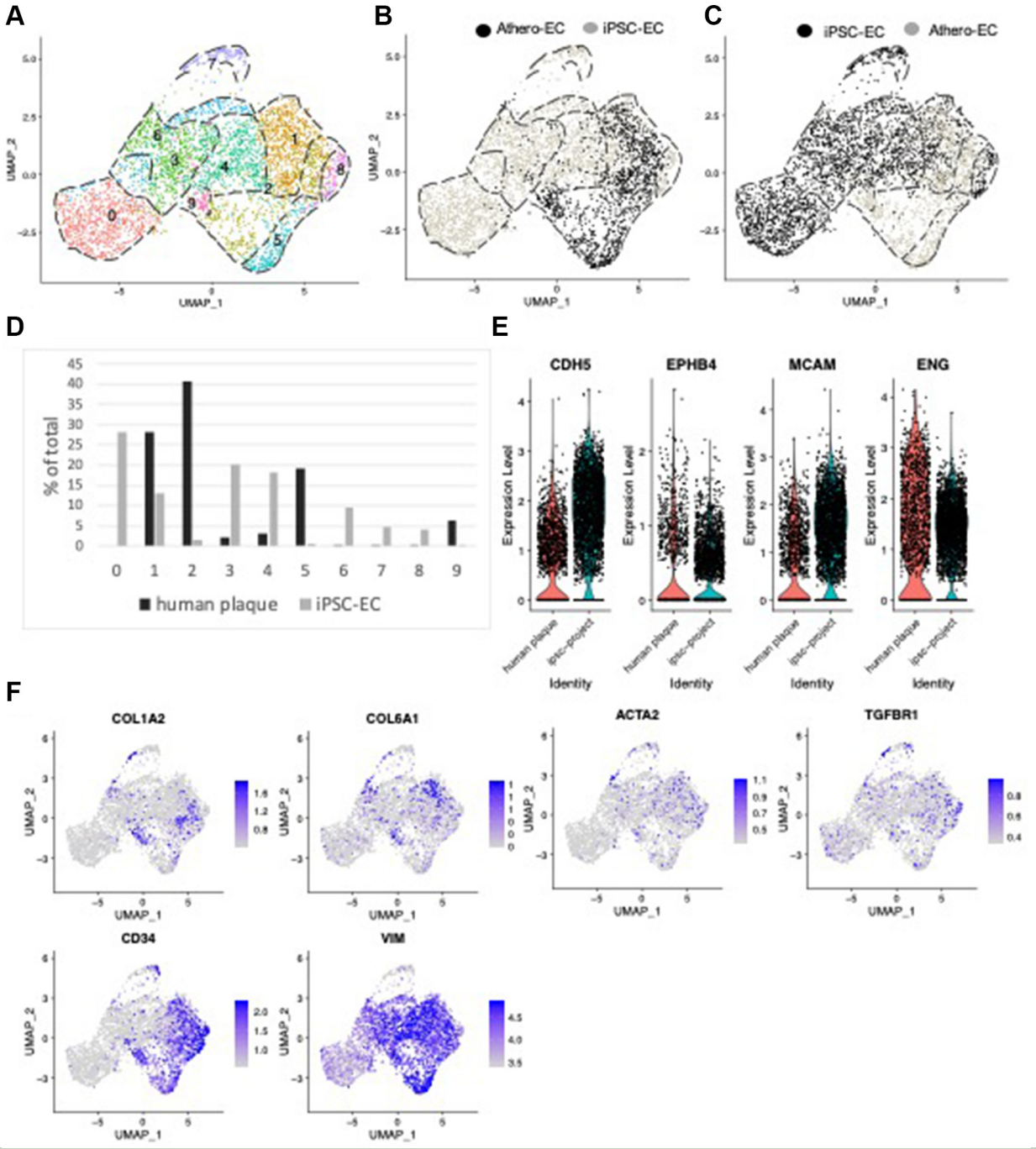

Supplementary Fig 5. Induced pluripotent stem cells directed to endothelial identity (*iPSC-ECs*) cluster together with human atherosclerosis-derived ECs. Human carotid atherosclerotic plaque single cell RNA sequencing (scRNA-seq) data from Pan et al were subset for CDH5^{+}, PECAM1 (CD31)$^{+}$ cells (1210 cells total) and clustered together with scRNA-seq data from aged hyperoxic iPSC-ECs using integrated multimodal analysis in Seurat. **(A)** UMAP showing 10 clusters. **(B)** human carotid plaque EC highlighted in black show overlap in clusters 1-4. **(C)** Graph in **(B)** reversed to visualize iPSC-ECs. **(D)** Quantification of the fraction of each cluster contributed to by iPSC-EC vs human plaque ECs, with overlap in clusters 1-4. **(E)** Violin plots showing similar expression of endothelial and pluripotency markers between human plaque EC and iPSC-EC. **(F)** Feature plots highlighting the expression of genes involved in endoMT and CD34 in overlapping clusters 1-4.